https://doi.org/10.15407/ujpe68.3.162

H.M. DLSHAD,[1] A.H. FATAH[2]

[1] General directorate of education, Sulaimaniyah
(Kurdistan-Iraq; e-mail: hawar.muhamaddlshad@gmail.com)
[2] Physics department, College of Science, University of Sulaimani, Sulaimaniyah
(Kurdistan-Iraq)

COMPARISON BETWEEN THE THEORETICAL CALCULATION OF COULOMB FORM FACTORS AND EXPERIMENTAL DATA FOR ^{12}C AND ^{20}Ne NUCLEI

The Coulomb form factors for the elastic and inelastic electron-nucleus scatterings have been calculated for ^{12}C and ^{20}Ne nuclei in the ground and excited states with the same parity. We use a microscopic theory involving the effects from high configurations outside the model space, which are called the Core Polarization (CP) effects. For the core polarization matrix elements, the realistic Michigan sum of the three-range Yukawa (M3Y) interaction and the Modified Surface Delta Interaction (MSDI) are used as the two-body interactions. Additionally, the Harmonic Oscillators (HO) potential is applied to calculate wave functions. In the final step, a comparison has been made between the theoretical calculations of Coulomb form factors based on (M3Y) and (MSDI) interactions and the available experimental data. It is noticed that the Coulomb form factors for the (M3Y) interaction give a sensible delineation of the measured data.

Keywords: inelastic scattering, Coulomb form factor, harmonic oscillator, wave function, core polarization effect.

1. Introduction

Electron scattering is considered as an efficient tool for examining the structure of nuclei and nucleons. The biggest advantage of the use of electrons is in that they can be broadly produced within the research facility, and since they are charged, and they can promptly be accelerated [1]. Furthermore, the main interaction between an electron and the target nucleus is well understood in the framework of Quantum Electrodynamics (QED) [2]. The origin of the other reason that the electron scattering is a valuable method for examining the properties of nuclear structures comes from its ability to identify the excited states, spins, and parities through the calculations of the reduced matrix elements of nuclear transitions. Thus, a comparison between the electron scattering form factors obtained from the experimental measurements and the ones obtained from theoretical calculations can contribute to a stringent test to approve the structural properties of the studied nuclei [3].

Various microscopic theories have been developed to study excitations in nuclei throughout the electron scattering process. One of these models is a shell model with restricted Model Space (MS), which succeeded in representing the static properties of nuclei like the nuclear mass, size, spin, and electric and magnetic moments [4]. The shell model is one of those models that have been adopted to describe the nuclear structure, and it is quite successful, particularly, to describe the closed-shell nuclei, light, and near closed-shell nuclei [5]. The data on the electron scattering can not be reproduced using only the model space wave functions in the form factor calculations. [6]. Therefore, the role of a core polarization, which affects out of the Model Space, is necessary to be included in the calculations. The Core Polarization is a process that has been so important in determining the two-particle effective shell model interaction.

There have been many residual interactions for the Core Polarization that were reported in the lit-

Citation: Dlshad H.M., Fatah A.H. Comparison between the theoretical calculation of Coulomb form factors and experimental data for ^{12}C and ^{20}Ne nuclei. *Ukr. J. Phys.* **68**, No. 3, 162 (2023). https://doi.org/10.15407/ujpe68.3.162.
Цитування: Длшад Х.М., Фатах А.Х. Порівняння теоретичного розрахунку кулонівських формфакторів та експериментальних даних для ядер ^{12}C і ^{20}Ne. *Укр. фіз. журн.* **68**, №3, 162 (2023).

erature such as the Modified Surface Delta Interaction (MSDI) [7] and Michigan Three-Range Yukawa (M3Y) Interaction [8]. The Core Polarization is a method for generating long-range correlations in a nucleus, beginning with a short-range interaction [9]. The concept of Core Polarization was generally applied in nuclear-structure calculations by Kuo and Brown [10] and many others starting in the late 1960s with abundant success. It is observed that the Core Polarization (CP) effects were extremely valuable, because it is very attractive in verifying the agreement between theory and experiment.

The first theory concerning the inelastic electron scattering was developed by Snedden and Touschek [11]. Later, the electron scattering including a form factor was first considered by Lyman *et al.* [12]. They had found the first experiment that was sensitive to the nuclear size. The nuclear size could be calculated by multiplying the nuclear form factor by Mott's cross-section. This form factor depends on the charge, current, and magnetization distribution in the nucleus.

Lukyanov *et al.* [13] calculated the elastic form factor for ^{12}C in the plane-wave Born approximation and by accounting for distortions of the electron wave's by the Coulomb field. They numerically solved the Dirac equation in the calculation.

In recent years, Jassim and Sahib [14] studied C_2 and C_4 Coulomb form factors of ^{18}O, ^{20,22}Ne nuclei. The Tassie and Bohr–Mottelson collective models were used to calculate core polarization effects. The wave functions are computed with three potentials: Harmonic oscillator (HO), Wood–Saxon (WS), and SKyrme (SKX).

Currently, the inelastic Coulomb electron scattering form factors for ^{64,66,68}Zn have been calculated by Salman *et al.* [17]. The HO potential has been adopted to compute the radial wave functions of single-particle matrix elements. To obtain the results, the following shell model codes were used: CP and NUSHELL.

The main goal of the present work is to compute the theoretical Coulomb form factors for ^{12}C and ^{20}Ne nuclei. To do this, by considering the role of the Model Space (MS) with the Core Polarization (CP) effects with each Modified Surface Delta Interaction (MSDI), and realistic interaction Michigan three-range Yukawa (M3Y), we chose the harmonic oscillator wave function as a single-particle one. Eventually, we will discuss the comparison between theoretical results and experimental data which are taken from other papers.

2. Theoretical Framework

In the framework of the Plane-Wave Born Approximation (PWBA), the squared form factor $|F_J^\eta(q)|^2$ of a given multipolarity (J) is a function of the momentum transfer (q) and can be written in terms of doubly reduced matrix elements (in a spin-isospin state) of the transition operator [2]:

$$|F_J(q)|^2 = \frac{4\pi}{Z^2(2j_i+1)}\left|\langle J_f T_f|||\hat{T}_{JT}|||J_i T_i\rangle\right|^2. \quad (1)$$

Here, J_i and J_f are the initial and final nuclear spins, respectively, T_i and T_f are the respective initial and final isospin states, where $T = 0$ or 1 for isoscalars or isovectors, $\hat{T}_{JT}$ represents the multipole operator with multipolarities JT, and Z is the atomic number.

The reduced matrix elements can be expressed in two parts; the first one is the Model Space (MS) matrix element and the second one is the Core Polarization (CP) matrix element [16]. We have

$$\langle\Gamma_f|||\hat{T}_\Lambda^\eta|||\Gamma_i\rangle = \langle\Gamma_f|||\hat{T}_\Lambda^\eta|||\Gamma_i\rangle_{\rm MS} + \langle\Gamma_f|||\delta\hat{T}_\Lambda^\eta|||\Gamma_i\rangle_{\rm CP}, \quad (2)$$

where $\Gamma_i = J_i T_i$, $\Gamma_f = J_f T_f$, and the multipolarity $\Lambda = JT$.

The MS reduced matrix element $\langle\Gamma_f|||\hat{T}_\Lambda^\eta|||\Gamma_i\rangle_{\rm MS}$ is given by:

$$\langle\Gamma_f|||\hat{T}_\Lambda^\eta|||\Gamma_i\rangle_{\rm MS} =$$

$$= \sum_{\alpha\beta} {\rm OBDM}(\alpha,\beta,J,\tau_z)\langle\beta|||\hat{T}_\Lambda^\eta|||\alpha\rangle_{\rm MS}. \quad (3)$$

The CP reduced matrix element $\langle\Gamma_f|||\delta\hat{T}_\Lambda^\eta|||\Gamma_i\rangle_{\rm CP}$ is given by:

$$\langle\Gamma_f|||\delta\hat{T}_\Lambda^\eta|||\Gamma_i\rangle_{\rm CP} =$$

$$= \sum_{\alpha\beta} {\rm OBDM}(\alpha,\beta,J,\tau_z)\langle\beta|||\delta\hat{T}_\Lambda^\eta|||\alpha\rangle_{\rm CP}, \quad (4)$$

where α, β represent the initial and final single-particle states, respectively (isospin is included), and OBDM is the One-Body Density Matrix elements in the neutron-proton formalism.

The single-particle matrix element $\langle\beta|||\hat{T}^{\eta}_{\Lambda}|||\alpha\rangle_{\rm MS}$ is calculated from [18, 19]:

$$\langle\beta|||\hat{T}^{\eta}_{\Lambda}|||\alpha\rangle_{\rm MS}=\langle j_\beta|||Y_\Lambda|||j_\alpha\rangle\langle n_\beta l_\beta|||j_J(qr)|||n_\alpha l_\alpha\rangle_{\rm MS}. \tag{5}$$

The single-particle matrix element $\langle\beta|||\delta\hat{T}^{\eta}_{\Lambda}|||\alpha\rangle_{\rm CP}$ can be represented in first-order perturbation theory as [17]:

$$\langle\beta|||\delta\hat{T}^{\eta}_{\Lambda}|||\alpha\rangle_{\rm CP}=\left\langle\beta|||\hat{T}^{\eta}_{\Lambda}\frac{Q}{E_\beta-H_0}V_{\rm res}|||\alpha\right\rangle+$$
$$+\left\langle\beta|||V_{\rm res}\frac{Q}{E_\alpha-H_0}\hat{T}^{\eta}_{\Lambda}|||\alpha\right\rangle, \tag{6}$$

where E_β and E_α are the single-particle energies of the states β and α, respectively, the interaction of (MSDI) and (M3Y) are utilize for the residual interaction $V_{\rm res}$.

In Eq. (6), the right-hand side terms can be presenteded as [20, 21]:

$$\left\langle\beta|||\hat{T}^{\eta}_{\Lambda}\frac{Q}{E_\beta-H_0}V_{\rm res}|||\alpha\right\rangle=$$
$$=\sum_{\alpha_1,\alpha_2,\Gamma}\frac{(-1)^{\beta+\alpha_2+\Gamma}}{e_\beta-e_\alpha-e_{\alpha_1}+e_{\alpha_2}}(2\Gamma+1)\begin{Bmatrix}\alpha & \beta & \Lambda\\ \alpha_2 & \alpha_1 & \Gamma\end{Bmatrix}\times$$
$$\times\sqrt{(1+\delta_{\alpha_1\alpha})(1+\delta_{\alpha_2\beta})}\,\langle\alpha\alpha_1|V_{\rm res}|\beta\alpha_2\rangle\,\langle\alpha_2|||\hat{T}^{\eta}_{\Lambda}|||\alpha_1\rangle. \tag{7}$$

Two terms with α_1 and α_2 exchanged with all over minus sign.

The single-particle energies (e) are obtained from the Harmonic Oscillator potential [18]:

$$e_{nlj}=\left(2n+l-\frac{1}{2}\right)\hbar\omega+$$
$$+\begin{cases}-\dfrac{1}{2}(l+1)\langle f(r)\rangle_{nl} & \text{for}\quad j=l-\dfrac{1}{2},\\[2mm] \dfrac{1}{2}l\langle f(r)\rangle_{nl} & \text{for}\quad j=l+\dfrac{1}{2}\end{cases} \tag{8}$$

with

$$\langle f(r)\rangle_{nl}\approx-20A^{-\frac{2}{3}} \tag{9a}$$

$$\hbar\omega=45A^{-\frac{1}{3}}-25A^{-\frac{2}{3}}. \tag{9b}$$

The ground-state charge density for the form factors can be found from the formula [22]

$$\rho_f(\mathbf{r}-\mathbf{r}')=\frac{1}{\sqrt{\pi^3\Omega^6}}\,e^{-\frac{(\mathbf{r}-\mathbf{r}')^2}{\Omega^2}},\quad \Omega=0.6532\text{ fm}. \tag{10}$$

Now, for the normalized folded-charge density, the root-mean-square becomes:

$$\langle r^2\rangle_{\rm ch}=\frac{1}{Z}\int\rho_{0\tau_z}(\mathbf{r})\,\rho_f(\mathbf{r}-\mathbf{r}')\,r^2d^3r. \tag{11}$$

Now, we calculate the core polarization matrix element for the Coulomb form factors with the interactions M3Y and MSDI. The M3Y interaction has the form [16]:

$$V_{\rm M3Y}=V_{\rm c}+V_{\rm l.s}+V_{\rm ten}, \tag{12}$$

where $V_{\rm c}$, $V_{\rm l.s}$, and $V_{\rm ten}$ are used for the central term, spin-orbit term, and tensor term, respectively [16].

The MSDI interaction gives [16]

$$V_{\rm MSDI}=-4\pi A_T\delta(\mathbf{r}_1-\mathbf{r}_2)\delta(\mathbf{r}_1-\mathbf{R}_0)+B(\boldsymbol{\tau}_1\,\boldsymbol{\tau}_2)+C, \tag{13}$$

where, $\mathbf{r}_1$ and $\mathbf{r}_2$ are the position vectors of the two interacting particles, $\delta(\mathbf{r}_1-\mathbf{r}_2)$ and $\delta(\mathbf{r}_1-\mathbf{R}_0)$ are the Dirac delta functions, R_0 is the nuclear radius, ($R_0=$ $=1.2A^{1/3}$ fm), and A is the nuclear mass number [21].

3. Results and Their Discussion

The Core Polarization (CP) effects are calculated according to Eq. (6) with M3Y and MSDI interactions. A computer program (written in FORTRAN 2008) is used with the shell model code OXBASH to obtain the results. The (M3Y) parameters are from the SE interaction with Elliot parameters [23]. The MSDI strength parameters have isospin representation and represented by A_T, B, and C, where T indicates the isospin equal to 0 or 1. These parameters are different for every nucleus, because they depend on the mass number of the nucleus, and we took them from Ref. [21]. The OBDM elements used in this paper are in the neutron-proton formalism. Moreover, the ground-state OBDM elements are found macroscopically by including the occupation numbers for neutrons and protons, but the OBDM for the excited states can be determined with OXBASH code [24]. The calculated root-mean-square (rms) charge

radii with the folding effect (effect of a proton size) are used for finding the elastic charge form factors.

In all graphs below, the form factors with Model Space and Core Polarization effects including the realistic M3Y interactions are the dashed curves, the form factors with MSDI as residual interaction are presented by solid curves, and the small filled circles represent the experimental values for the electron scattering form factors.

3.1. Carbon nucleus ^{12}C

The carbon nucleus could be a particularly engaging target for such studies, as one can specifically test protons from specific nuclear shells, s and p [27]. Three isotopes of carbon exist naturally, ^{12}C and ^{13}C being stable, while ^{14}C is a radionuclide. The isotope carbon-12 (^{12}C) forms 98.93% of the carbon on the Earth. Therefore, we choose it for our work. The structure of stable carbon nucleus ^{12}C consists of six protons and six neutrons. It has eight nucleons outside the closed core He^4 nucleus distributed over ($1p3/2$, $1p1/2$). They are four protons and four neutrons in the Model Space. Under the electro-excitation, the nucleus is excited from the ground state (0^+0) to the excited state (2^+0) with the energy $E = 4.4$ MeV [28]. That means only one transition from the ground state is investigated. The Harmonic Oscillator size parameter is $b = 1.692$ fm [29]. This parameter plays a role in determining the form factor. Here, the squared Coulomb form factors are plotted as functions of the momentum transfer (q). With the multipolarities, $J = 2$ of C_2 transition.

3.1.1. Elastic Coulomb form factors for (0^+0) state

Based on the structure of the ^{12}C nucleus, Table 6 summarizes the calculated rms for the ground state with $J^\pi T = 0^+0$ and without folding. To calculate the C_0-multipole, the values of OBDM elements are taken into account. Table 1 lists them. In Fig. 1, the experimental data on the C_0 Coulomb form factors are compared with the theoretical calculations. It was noticed that the calculation of form factor with the realistic interaction (M3Y) very well describes the experimental data for the whole momentum transfer interval. In contrast, the calculation with MSDI has few similarities with the measured data in the momentum transfer regions ($q \geq 3$ fm^{-1}).

3.1.2. Inelastic Coulomb form factor for 2^+0 state

For the isoscalar transition (2^+0) with energy $E = 4.4$ MeV, the calculated Coulomb coefficients C_2 are plotted as a function of the momentum transfer (q) for the transitions. The theoretical electron scattering form factors with CP effects using MSDI and M3Y interactions with the measured data are displayed in Fig. 2, where the OXBASH code used to evaluate OBDM is given in Table 2. As can be observed, the calculation with (M3Y) brings the theoretical results closer to the experimental ones at the interval of momentum transfers ($0.5 \leq q \leq 2$ fm^{-1}), while, in the current study, the calculation with MSDI is overestimated at ($q \leq 1.5$ fm^{-1}), but it is extremely interesting in the interval ($1.5 \leq q \leq 2$ fm^{-1}), where the calculation fits the data perfectly.

3.2. Neon nucleus ^{20}Ne

There are three stable isotopes of neon: ^{20}Ne, ^{21}Ne, and ^{22}Ne. In addition, 17 radioactive isotopes ranging from ^{15}Ne to ^{34}Ne, all of which being short-lived, have been discovered. ^{20}Ne is a well-known example, because it forms (90.48%) of a neon gas and

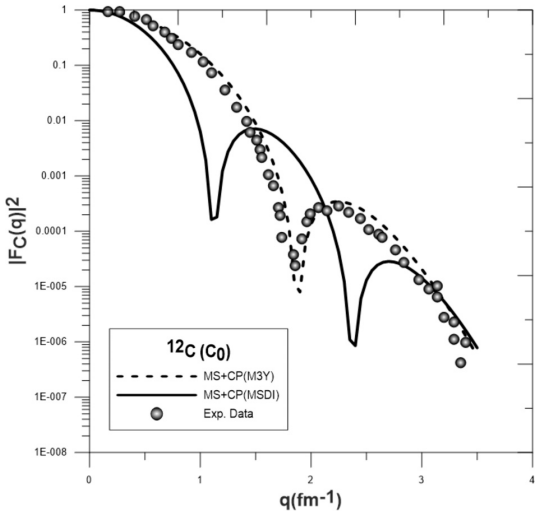

Fig. 1. Ground state Coulomb form factors for ^{12}C. The data were taken from Ref. [28]

Table 1. **The calculated OBDM elements for the Coulomb C_0 transition of ^{12}C**

j_1	j_2	OBDM(n)	OBDM(p)
1 $S1/2$	1 $S1/2$	1.4142	1.4142

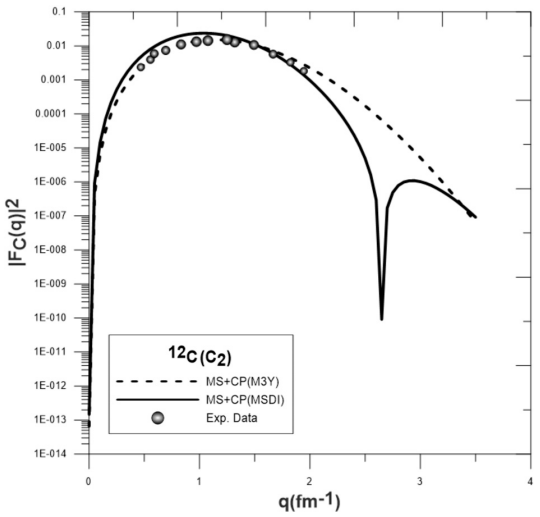

Fig. 2. Inelastic C_2 Coulomb form factors for 2^+0 state of ^{12}C with $E = 4.4$ MeV. The experimental data were taken from Ref. [30]

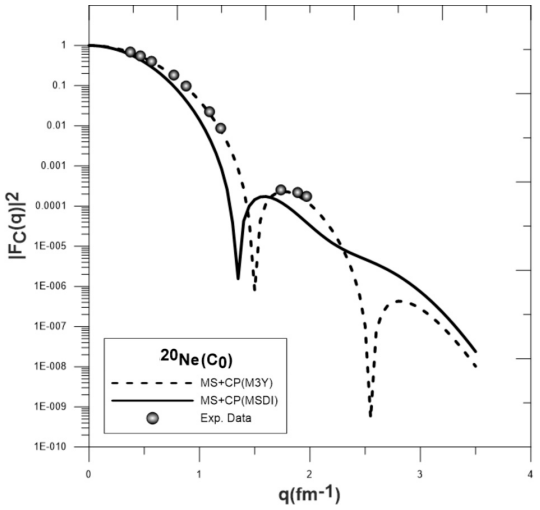

Fig. 3. Ground state Coulomb form factors for ^{20}Ne. The data were taken from Ref. [32]

a nearly inert noble gas. It consists of ten protons and ten neutrons. The nucleons of the core (^{16}O) are eight protons and eight neutrons which are inert in the $(1s1/2, 1p3/2, 1p1/2)$ $J = 0, T = 0$ configuration, and the remaining nucleons are distributed over all possible combinations of the ($1d5/2$, $2s1/2$, $1d3/2$) orbits according to the Pauli exclusion principle [31]. There are two protons and two neutrons in the Model Space. We present here some results concerning the ground state ($J^\pi T = 0^+0$), excitation states ($J^\pi T = 2^+0$) and $E = 1.63$ MeV for C_2 transition and ($J^\pi T = 4^+0$) $E = 4.25$ MeV [32] for the C_4 transition of ^{20}Ne for which the data have been recently measured. The squared form factors are plotted with the transferred momentum. In addition, the parity of these transitions remain constant, and with a Harmonic Oscillator size parameter $b = 1.869$ fm [33].

3.2.1. Elastic Coulomb form factor for (0^+0) state

The elastic Coulomb form factors of ^{20}Ne nucleus with $J^\pi T = 0^+0$ are presented in Fig. 3. The OBDM elements for the ground state were calculated with the effect of occupation numbers and are displayed in Table (3). Furthermore, the computed ground-state root-mean-square charge radii are demonstrated in Table 6. The results with the Core Polarization interaction M3Y, as shown in the figure, are in marginally better agreement with the experimental data of the other workers for the momentum transfer regions ($0.4 \leq q \leq 2.0$ fm^{-1}), but the approximation with the experimental data at high values of q is poor. On the other hand, the form factors with MSDI interaction underestimate the data along with all momentum transfer points.

3.2.2. Inelastic Coulomb form factor for 2^+0 state

In this state, the nucleus ^{20}Ne is excited from the ground state (0^+0) to the excited state (2^+0) with the excitation energy of 1.63 MeV. By applying the parity and angular momentum selection rules, one

Table 2. **The calculated OBDM elements for the Coulomb C_2 transition of ^{12}C**

j_1	j_2	OBDM(n)	OBDM(p)
$1P1/2$	$1P3/2$	0.5370	0.5370
$1P3/2$	$1P1/2$	–0.3545	–0.3545
$1P3/2$	$1P3/2$	–0.2192	–0.2192

Table 3. **The calculated OBDM elements for the Coulomb C_0 transition of ^{20}Ne**

j_1	j_2	OBDM(n)	OBDM(p)
$1S1/2$	$1S1/2$	1.4142	1.4142
$1P3/2$	$1P3/2$	2.0000	2.0000
$1P1/2$	$1P1/2$	1.4142	1.4142

can get the multipolarity C_2. The calculated C_2 form factors including the CP effect with M3Y and MSDI interactions are displayed in Fig. 4, and the evaluated OBDM elements are listed in Table 4. It is clear that the M3Y and MSDI results do not coincide completely with the low and high values of (q), but they both agree with the experimental data up to $(q = 2\ \text{fm}^{-1})$.

3.2.3. Inelastic Coulomb form factor for 4^+0 *state*

Here, the nucleus is excited by the electron from the ground state (0^+0) to the excited state (4^+0) with the excitation energy $E = 4.248$ MeV. We present it in Fig. 5. The OBDM elements evaluated with OXBASH code are displayed in Table 5.

The calculations include the Core Polarization effects with the M3Y and MSDI as residual interactions separately. At a momentum transfer of $(0.9 \leq \leq q \leq 2\ \text{fm}^{-1})$, both results lead to give an improvement in the measured Coulomb C_4 form factors. But, at the other position of (q), there is no measured data to be compared with the theoretical results.

Table 4. **The calculated OBDM elements for the Coulomb C_2 transition of ^{20}Ne**

j_1	j_2	OBDM(n)	OBDM(p)
$1d3/2$	$1d3/2$	–0.0620	–0.0620
$1d3/2$	$1d5/2$	0.0700	0.0700
$1d3/2$	$2s1/2$	0.1532	0.1532
$1d5/2$	$1d3/2$	–0.0591	–0.0591
$1d5/2$	$1d5/2$	–0.2836	–0.2836
$1d5/2$	$2s1/2$	–0.3204	–0.3204
$2s1/2$	$1d3/2$	–0.1049	–0.1049
$2s1/2$	$1d5/2$	–0.2698	–0.2698

Table 5. **The calculated OBDM elements for the Coulomb C_4 transition of ^{20}Ne**

j_1	j_2	OBDM(n)	OBDM(p)
$1d3/2$	$1d5/2$	0.2073	0.2073
$1d5/2$	$1d3/2$	–0.1772	–0.1772
$1d5/2$	$1d5/2$	–0.2904	–0.2904

Table 6. **The calculated and measured charge radii for the ground-state nuclei**

Charge radii in Fermi			
Nuclei	With folding	Without folding	Exp. [34]
^{6}Li	2.534	2.657	2.589
^{12}C	2.467	2.594	2.470
^{20}Ne	2.945	3.052	3.005

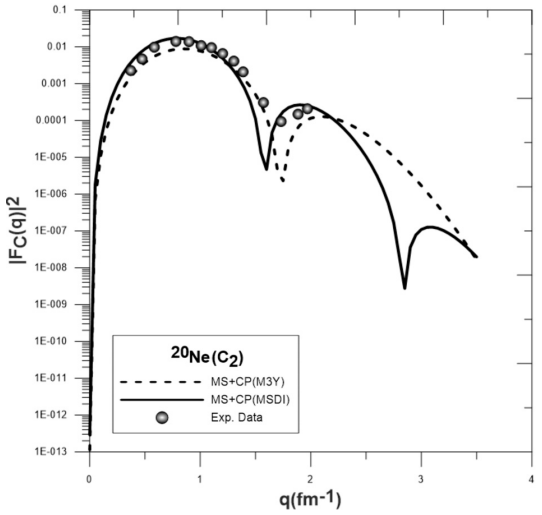

Fig. 4. Inelastic C_2 Coulomb form factors for 2^+0 state of ^{20}Ne with $E = 1.63$ MeV. The data were taken from Ref. [32]

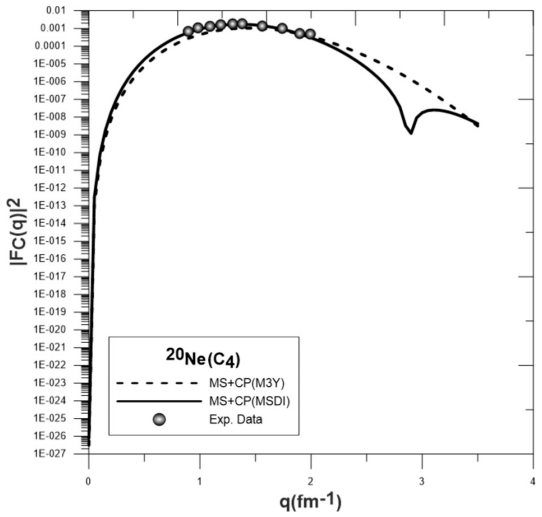

Fig. 5. Inelastic C_4 Coulomb form factors for 4^+0 state of ^{20}Ne with $E = 4.248$ MeV. The data were taken from Ref. [32]

4. Summary and Conclusions

In this work, we have calculated the Coulomb form factors for carbon-12 and neon-20 with two different methods. First of all, we made a theoretical calcula-

tion to find the form factors. The model out of the model space is used. It is known as the core polarization effect. The core polarization matrix elements are found by using M3Y and MSDI interactions. We compared our results with the original experimental data. For the nuclei under consideration, the degree of agreement between the calculated Coulomb form factors $F_{\rm C}(q)$ and those of the experimental data became better, when the Core Polarization effects with the M3Y interaction were involved. This is obvious for all Coulomb coefficients C_0 and coefficients C_2 transitions, because the M3Y interaction is a more realistic nucleon-nucleon interaction used in the CP calculation, whereas the MSDI interaction is dealing with the surface nucleons only. Thus, it is less compatible with the experimental data, particularly for ^{12}C nucleus. In the case of ^{20}Ne nucleus, for both the M3Y and MSDI interactions, the agreement of high multipolarity such as C_4 transitions are more clear than for C_2 transitions, when comparing with experimental results. This indicates that the HO wave function succeeded in representing the radial wave functions perfectly. Likewise, the calculated rms charge radii for the ground states of our nuclei show a very good agreement with the experimental data. There are many differences between our work and the works of other researchers. The main difference is in that we use the M3Y and MSDI interactions together. Moreover, we study both similarities and differences between the M3Y results and experiment, on one side, and the MSDI ones and experimental data, on the other side. These two nuclei ^{12}C and ^{20}Ne, which are used in our work, have never been studied before in this way.

The first author's M.Sc. thesis includes this work. The authors gratefully acknowledge the University of Sulaimani for their support in completing this study.

1. J.D. Walecka. *Electron Scattering for Nuclear and Nucleon Structure* (Cambridge University Press, 2001) [ISBN: 0-511-03483-0].
2. T. de Forest Jr, J.D. Walecka. Electron scattering and nuclear structure. *Adv. Phys.* **15**, 1 (1966).
3. A.A. Al-Sammarraie, M.L. Inche Ibrahim, M. Ahmed Saeed, F.I. Sharrad, H. Abu Kassim. Inelastic electric and magnetic electron scattering form factors of Mg nucleus: Role of factors. *Int. J. Mod. Phys. E* **26**, 1750032 (2017).
4. K.S. Jassim. The electron scattering form factor of ^{10}B, ^{32}S and ^{48}Ca nuclei. *Phys. Scr.* **86**, 035202 (2012).
5. A. Gottardo, J.J. Valiente-Dobón, G. Benzoni, R. Nicolini, A. Gadea, S. Lunardi, S. Pietri. New isomers in the full seniority scheme of neutron-rich lead isotopes: The role of effective three-body forces. *Phys. Rev. Lett.* **109**, 162502 (2012).
6. R.A. Radhi, A.A. Alzubadi. Study the nuclear form factors of low-lying excited states in nucleus using the shell model with skyrme effective interaction. *Few-Body Syst.* **60**, 57 (2019).
7. A.H. Taqi, R.A. Radhi. Longitudinal form factor of isoscalar particle-hole states in ^{16}O, ^{12}C and ^{40}Ca with M3Y interaction. *Turk. J. Phys.* **31**, 253 (2007).
8. J. Escher. *Electron Scattering Studies in the Framework of the Symplectic Shell Model* (Louisiana State University, 1997).
9. B.R. Barrett. Effective operators in nuclear-structure calculations. *J. Phys.: Conference Series* **20**, 48 (2005).
10. T.T.S. Kuo, G.E. Brown. Structure of finite nuclei and the free nucleon-nucleon interaction: An application to ^{18}O and ^{18}F. *Nucl. Phys.* **85**, 40 (1966).
11. I.N. Sneddon, B.F. Touschek. The excitation of nuclei by electrons. *Proc. Math. Phys. Sci.* **193**, 344 (1948).
12. E.M. Lyman, A.O. Hanson, M.B. Scott. Scattering of 15.7 Mev electrons by nuclei. *Phys. Rev.* **84**, 626 (1951).
13. V.K. Lukyanov, D.N. Kadrev, E.V. Zemlyanaya, A.N. Antonov, K.V. Lukyanov, M.K. Gaidarov, K. Spasova. Microscopic analysis of 11Li elastic scattering on protons and breakup processes within the ^{6}Li $+2n$ cluster model. *Phys. Rev.* **2**, 034612 (2013).
14. I.A.H. Ajeel, M.J.R. Aldhuhaibat, K.S. Jassim. Coulomb C2 and C4 Form Factors of ^{18}O, ^{20,22}Ne nuclei using Bohr–Mottelson collective model. *Ukr. J. Phys.* **67**, 110 (2022).
15. A.D. Salman, S.A. Al-Ramahi, M.H. Oleiwi. Inelastic electron-nucleus scattering form factors for ^{64,66,68}Zn isotopes. *AIP Conf. Proc.* **2144**, 030029 (2019).
16. E.M. Raheem, R.O. Kadhim, N.A. Salman. The effects of core polarisation on some even–even sd-shell nuclei using Michigan three-range Yukawa and modified surface delta interactions. *Pramana* **92**, 39 (2019).
17. A.D. Salman, D.R. Kadhim. Longitudinal electron scattering form factors for ^{54,56}Fe. *Int. J. Mod. Phys. E* **23**, 1450054 (2014).
18. B.A. Brown, R. Radhi, B.H. Wildenthal. Electric quadrupole and hexadecupole nuclear excitations from the perspectives of electron scattering and modern shell-model theory. *Phys. Rep.* **101**, 313 (1983).
19. A.H. Fatah, R.A. Radhi, N.R. Abdullah. Analytical derivations of single-particle matrix elements in nuclear shell model. *Comm. Theo. Phys.* **66**, 104 (2016).
20. A.D. Salman, N.M. Adeeb, M.H. Oleiwi. Core polarization effects on the inelastic longitudinal C2 and C4 form factors of ^{46,48,50}Ti nuclei. *J. Adv. Phys. part. phys.* **3**, 20 (2013).
21. P.J. Brussaard, P.W.M. Glaudemans, P.W.M. Glaudemans. *Shell-Model Applications in Nuclear Spectroscopy* (North-Holland publishing company, 1977).

22. T. Suda, H. Simon. Prospects for electron scattering on unstable, exotic nuclei. *Pro. Part. Nucl. Phys.* **96**, 1 (2017).
23. G. Bertsch, J. Borysowicz, H. McManus, W.G. Love. Interactions for inelastic scattering derived from realistic potentials. *Nucl. Phys. A* **284**, 399 (1977).
24. S. Mohammadi, B.N. Giv, N.S. Shakib. Energy levels calculations of ^{24}Al and ^{25}Al isotopes. *Nucl. Sci.* **2**, 1 (2017).
25. J.C. Bergstrom, S.B. Kowalski, R. Neuhausen. Elastic magnetic form factor of ^{6}Li. *Phys. Rev. C* **25**, 1156 (1982).
26. J.C. Bergstrom, U. Deutschmann, R. Neuhausen. Electron scattering from the 3.65 MeV (0+, $T = 1$) state in 6Li at high momentum transfer. *Nucl. Phys. A* **327**, 439 (1979).
27. T. Brecelj, S.J. Paul, T. Kolar, P. Achenbach, A. Ashkenazi, R. Böhm, C. Giusti. Polarization transfer to bound protons measured by quasielastic electron scattering on ^{12}C. *Phys. Rev. C*, **101**(6), 064615 (2020).
28. I. Sick, J.S. McCarthy. Elastic electron scattering from ^{12}C and ^{16}O. *Nucl. Phys. A* **150**, 631 (1970).
29. C.W. De Jager, H. De Vries, C. De Vries. Nuclear charge- and magnetization-density-distribution parameters from elastic electron scattering. *At. Data Nucl. Data Tables* **14**, 479 (1974).
30. J.B. Flanz, R.S. Hicks, R.A. Lindgren, G.A. Peterson, A. Hotta, B. Parker, R.C. York. Convection currents and spin magnetization in E2 transitions of ^{12}C. *Phys. Rev. Lett.* **41**, 1642 (1978).
31. S. Mohammadi, M. Mounesi. Energy levels calculations of 30 Si and 31 Si isotopes using OXBASH code. *Americ. J. Mod. Phys.* **4**, 36 (2015).
32. Y. Horikawa. Deformations of Ground-Bands in Ne_{20}, Mg_{24} and Si_{28}. I. *Prog. Theo. Phys.* **47**, 867 (1972).
33. B.A. Brown, W. Chung, B.H. Wildenthal. Electromagnetic multipole moments of ground states of stable odd-mass nuclei in the sd shell. *Phys. Rev. C* **22**, 774 (1980).
34. I. Angeli, K.P. Marinova. Table of experimental nuclear ground state charge radii. *An update, At. Data Nucl. Data Tables* **99**, 69 (2013).

Received 30.09.22

Х.М. Длшад, А.Х. Фатах

ПОРІВНЯННЯ ТЕОРЕТИЧНОГО РОЗРАХУНКУ КУЛОНІВСЬКИХ ФОРМФАКТОРІВ ТА ЕКСПЕРИМЕНТАЛЬНИХ ДАНИХ ДЛЯ ЯДЕР ^{12}C І ^{20}Ne

Розраховано кулонівські формфактори для пружного і непружного розсіювання електронів на ядрах ^{12}C і ^{20}Ne в основному чи збуджених станах однієї парності. Застосовано мікроскопічну теорію, яка містить ефекти від вищих конфігурацій за межами модельного простору, що мають назву ефекти поляризації кора. Для знаходження елементів матриці поляризації кора двочастинкова взаємодія представлена реалістичною Мічіган взаємодією у вигляді лінійної комбінації трьох потенціалів Юкави різного радіусу (M3Y), або модифікованою поверхневою дельта-взаємодією (MSDI). Додатково в розрахунках хвильових функцій використано потенціал гармонічного осцилятора. Теоретичні результати, отримані на базі M3Y та MSDI, порівняно з експериментальними даними. Ми зауважуємо, що кулонівські формфактори, обчислені із взаємодією M3Y, краще описують експериментальні дані.

Ключові слова: непружне розсіювання, кулонівський формфактор, гармонічний осцилятор, хвильова функція, ефект поляризації кора.